POLARIZATION OF LOOP-TOP AND FOOTPOINT SOURCES IN MICROWAVE BURSTS

Y. N. SU[1,2] and G. L. HUANG[1]
[1]*Purple Mountain Observatory, Nanjing 210008, China*
[2]*The Graduate School of the Chinese Academy Sciences, China*

(Received 8 September 2003; accepted 30 October 2003)

Abstract. The polarization is analyzed in four microwave bursts with one loop-top and two footpoint sources observed at 17 GHz with the Nobeyama Radioheliograph (NoRH). The loop-like structure of the four events is confirmed by simultaneous SOHO/MDI magnetograms and TRACE/EUV images or *Yohkoh*/SXT images. The heliocentric distance of the four events is greater than 30°. The three microwave sources in each given burst are polarized in the same sense. This may be interpreted in terms of extraordinary mode emission, taking into account the polarity of the underlying magnetic field and propagation effects, which may lead to inversion of the sense of polarization in the limbward foot and loop-top source of the flaring loop.

1. Introduction

The observed polarization of the microwave emission from a magnetoactive plasma is determined by two factors: intrinsic polarization in the source region, and propagation effects. The intrinsic polarization is determined by the predominant emission mode, and the polarization characteristics of that particular mode.

The computation of the gyro-synchrotron (g-s) emission is well known (Ramaty, 1969; Takakura and Scalise, 1970; Takakura, 1972). Here, τ is the optical thickness along the line of sight. They showed that at high frequencies with $\tau < 1$, the predominant emission mode is extraordinary mode (*e*-mode), but it becomes ordinary mode (*o*-mode) at the lower frequencies with $\tau > 1$. Preka-Papadema and Alissandrakis (1988) showed that due to thermal gyro-resonance (g-r) absorption at the third harmonic, the suppression of *e*-mode emission, originating in the lower layers of the loop, will produce excess *o*-mode radiation at the diskward foot of a flaring loop. This requires that the magnetic field is strong enough to bring the third harmonic layer inside the flaring loop.

Alissandrakis, Nindos, and Kundu (1993) have found evidence for ordinary mode emission in two classes of events. In one class the *o*-mode comes from the regions overlying the strong magnetic field, which can be interpreted in terms of the thermal g-r absorption at the third harmonic. In the other class the entire burst emits in the *o*-mode, which may be attributed to high g-s optical depth.

Several authors have studied the effects of wave propagation (Cohen, 1960; Zheleznyakov and Zlotnik, 1963; Bandiera, 1982). A circularly polarized wave

Solar Physics **219:** 159–168, 2004.

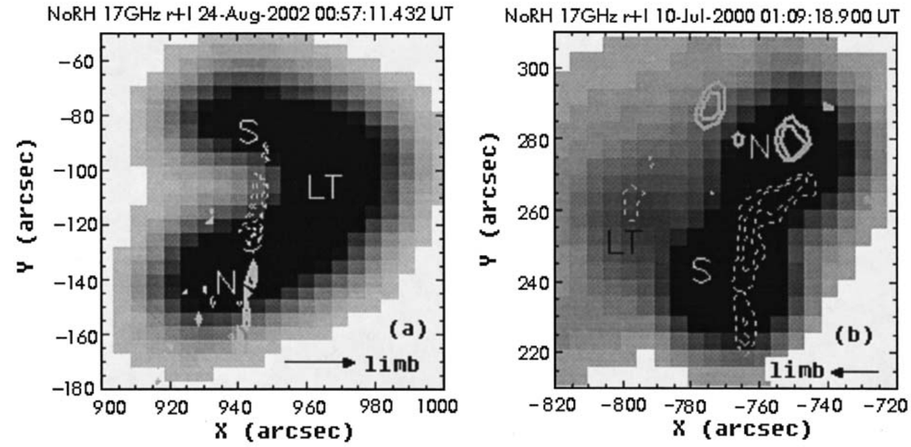

Figure 1. (a) The photospheric magnetic field (SOHO/MDI) of event 1 with contours 250, 150, −300, −250 G overlaid on the Stokes *I* image at 17 GHz with NoRH. The *solid* and *dashed lines* are for positive and negative values, respectively. (b) Event 2. Similar to (a), the contours: 600, 400, −1000, −800 G.

has its sense of rotation reversed when propagating through a quasi-transverse (QT) region, and the mode coupling is weak. If the mode coupling is strong, the polarization sense is constant. Alissandrakis and Preka-Papadema (1984, Paper I) presented a model for illustrating the propagation effects on the radiation emitted by a flare loop, which is located 30° away from the solar disk center (Figure 4 in Paper I). A TF line is defined as the loci of points where the magnetic field is perpendicular to the direction of wave propagation. The TF line will divide the loop into two parts, i.e., diskward and limbward sides. The radiation from the limbward side will cross the TF line, then the sense of polarization will be inverted, if the mode coupling is weak.

Alissandrakis, Nindos, and Kundu (1993) analyzed the polarization of the footpoints in simple microwave bursts at 4.9 GHz with the Westerbork Synthesis Radio Telescope. However, a detailed analysis is still needed for propagation effects and predominant emission mode of loop-top and footpoint sources in microwave bursts. In this paper simultaneous microwave and EUV or soft X-ray data, together with photospheric magnetograms are used to identify the magnetic geometry, which will be used to interpret the polarization characteristics of the flares.

The comparison of the microwave emission between the loop-top and footpoint sources has been studied (Paper I; Klein and Trottet, 1984; Melnikov, Shibasaki, and Reznikova, 2002).

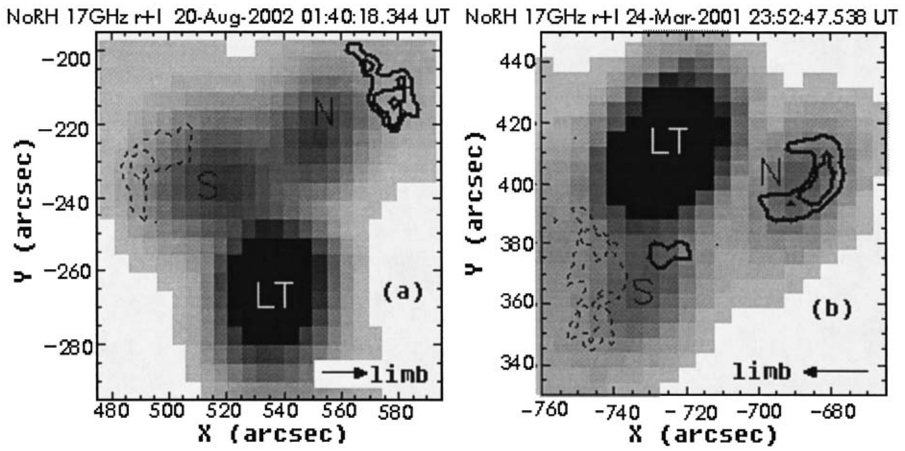

Figure 2. Similar to Figure 1. (a) Event 3 contours: 1150, 1000, −1650, −1300 G. (b) Event 4 contours: 1200, 800, −550, −410 G.

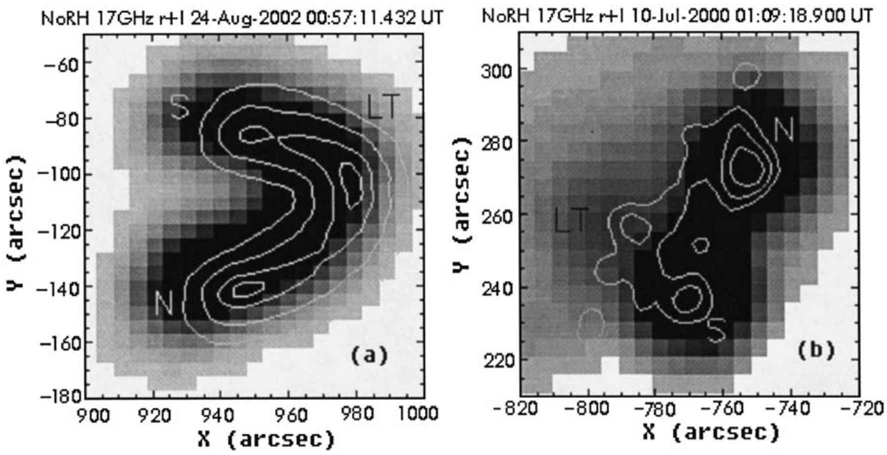

Figure 3. Stokes *I* (NoRH) at 34 GHz with contours overlaid on the NoRH/17GHz I image. (a) Event 1 contours: 5.e4, 5.e5, 2.2e6, 3.6e6. (b) Event 2. contours: 5.e4, 9.e4, 1.5e5.

2. Observations

Four flares are selected for a detailed study of the spatial properties of microwave emission from a flare loop: 24 August 2002 (event 1), 10 July 2000 (event 2), 20 August 2002 (event 3), and 24 March 2001 (event 4), which are characterized by one loop-top and two footpoint sources observed at 17 GHz with the Nobeyama Radioheliograph (NoRH). The Stokes *I* image at 17 GHz is selected at a given time *T* in order to obtain a clear image with triple source structure. There are two sub-sources of each flare at 17 GHz corresponding to the two opposite polarities of the magnetic field in the SOHO/MDI image, so they may refer to the footpoints (FP), and the third may be the loop-top source (LT) (Figures 1 and 2). According

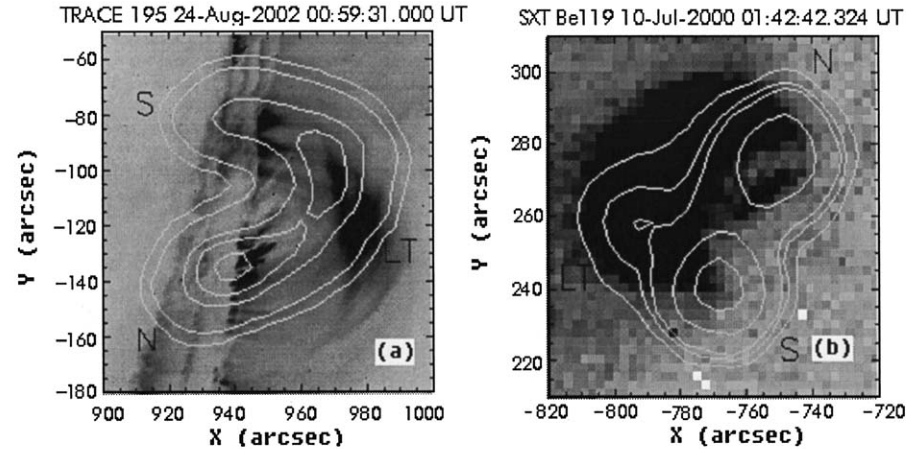

Figure 4. (a) Event 1 NoRH/17 GHz I with contours: 8.e5, 2.e6, 1.e7, 1.6e7, 2.5e7 overlaid on the EUV image. (b) Event 2 NoRH/17 GHz I with contours: 1.e5, 2.e5, 2.96e5, 1.e6, 2.5e6 overlaid on the soft X-ray image.

to the comparison of the brightness temperature between the LT and FP, the four events are divided into two types.

Events 1 and 2 are classified as type I flares, (GOES classification X3.1 and C6.0, respectively). A loop-like structure can be seen from the Stokes I image at 17/34 GHz and the EUV image or the soft X-ray image (Figures 3 and 4). For event 1, only two footpoints can be seen at 17 GHz in the early rising phase, the LT appears later and only one foot is brighter than the LT near the maximum time (Figure 4(a)). The microwave brightness temperature at 17 GHz of the FP for event 2 is always higher than that of the LT during the impulsive phase like the situation in Figure 4(b). The time profiles of flux at 17 GHz of the two events obtained with the Nobeyama Radio Polarimeters (NoRP) are shown in Figure 5. The time profiles show that the two flares are impulsive ones. The microwave spectra at a given time T obtained with the NoRP data are shown in Figure 5.

Events 3 and 4 are flares of type II, and flare 3 is an M5.0 event for the GOES soft X-ray class. A triple-source structure for the two events can be seen from the Stokes I image at 17 GHz. A single strong source of events 3 seen from the Stokes I image at 34 GHz and EUV image is located at the loop top (Figure 6). A very weak source for flare 4 can be seen from the microwave image at 34 GHz and EUV image. The LT of events 3, 4 is always brighter than the FP at 17 GHz during the impulsive phase as shown in Figure 2. The time profiles at 17 GHz of the two events are complicated. The microwave spectra at time T are shown in Figure 7.

However, the polarization sense in each type is different. The LT and FP of events 1, 4 are both polarized in the right circular polarization (RCP) sense (Figures 8(a) and 9(b)). For events 2, 3, the polarization sense of the three sources is left circular polarization (LCP) (Figures 8(b) and 9(a)).

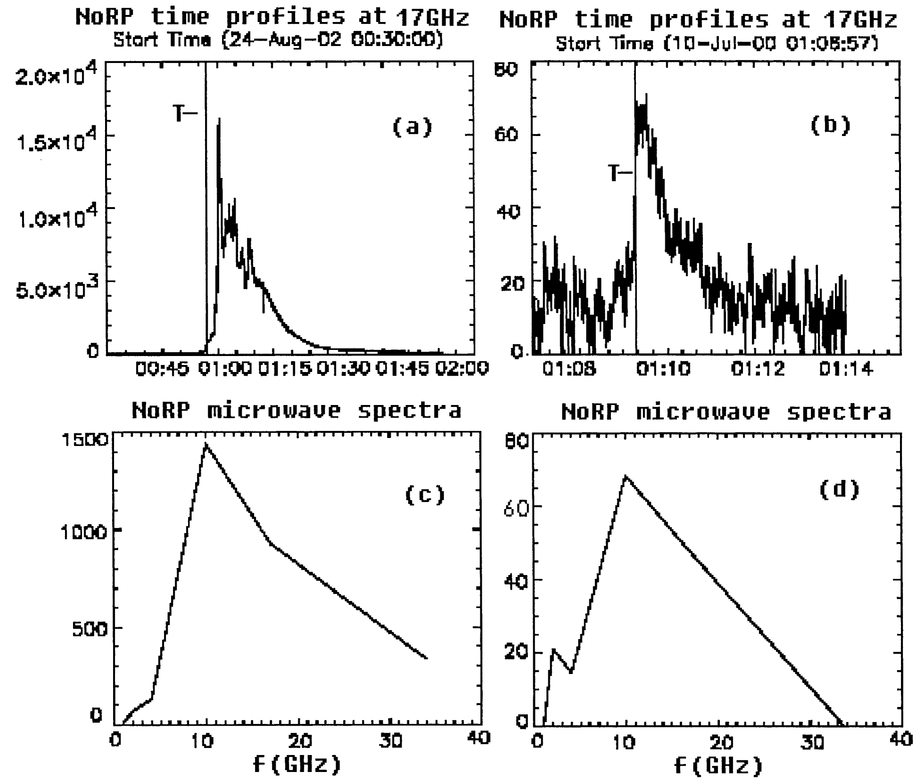

Figure 5. (a), (b) The time profiles of flux at 17 GHz from NoRP for events 1, 2, the *vertical line* marks the time T when the NoRH images are given. (c), (d) The microwave spectra from NoRP of events 1, 2 at time T.

3. Discussion

3.1. Intrinsic Polarization Mode

From the microwave spectra obtained using the NoRP data, we find that the microwave emission of flares 1, 2, and 4 at 17 GHz is from an optically thin radio source. Figure 7(c) shows that the peak frequency is roughly 17 GHz, and so the 17 GHz emission is not optically thin in event 3. Brightness temperature of both FP is significantly weak as compared with that of the LT. So the microwave spectrum (Figure 7(c)), which is derived from the total flux measurements, is applicable only to the LT. And the 17 GHz emission is probably optically thin in both FP. For the LT, *e*-mode emission may also predominant, because *o*-mode emission prevails only at a lower frequency in the optically thick source.

In a region where a strong magnetic field is present, the absorption coefficient for radio waves is determined by the resonance absorption at harmonics of the gyro-frequency (Lara *et al.*, 1998). For the frequency 17 GHz, the necessary mag-

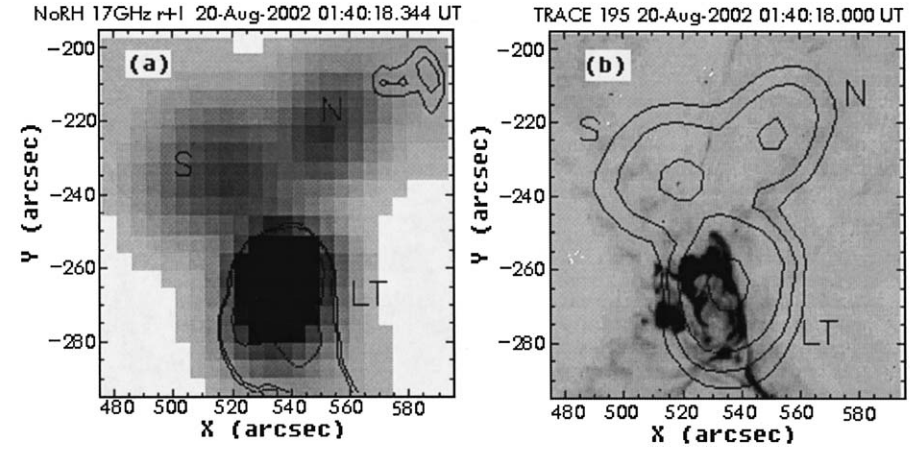

Figure 6. Event 3. (a) NoRH/34GHz I with contours: 3.e4, 3.5e4, 9.6e4, 2.8e5, 6.5e5 overlaid on the NoRH/17GHz I image. (b) NoRH/17G I with contours: 1.4e5, 2.8e5, 6.3e5, 3.e6 overlaid on the TRACE/EUV image.

netic field strengths for the 2nd, 3rd and 4th harmonics are 3035.71, 2023.81, and 1517.86 G, respectively. These magnetic field strengths are not reasonable, because they are rather high compared with the maximum photospheric magnetic field (300 –1200 G in the four flares observed by SOHO/MDI). Then the conclusion of suppression of *e*-mode emission due to thermal g-r absorption at the third harmonic is not true for all four flares.

From the discussion above, *e*-mode is the predominant emission mode of the four flares.

3.2. Propagation Effects

3.2.1. *QT Region*

In our case the QT approximation holds only a very narrow range of angle θ in the vicinity of $\pi/2$; here θ is the angle between the direction of wave propagation and magnetic field. The theory of magnetoionic mode coupling by Cohen (1960) is extended to the case in which the superposed magnetic field varies in amplitude and direction. Calculations are limited to high frequencies and to the case of a medium stratified in planes parallel to the wave front. In QT regions the coupling may be much stronger because the characteristic polarizations change rapidly with θ. The QT transitional frequency f_t is given

$$f_t^4 = 10^{17} N_e S B^3. \tag{1}$$

Here, f is the observation frequency, N_e is the electron density, B is the magnetic field strength, S is the scale length for change of the direction of the magnetic field. The modes are weakly or strongly coupled according to whether $f^4 \ll f_t^4$ or $f^4 \gg f_t^4$ (Cohen, 1960).

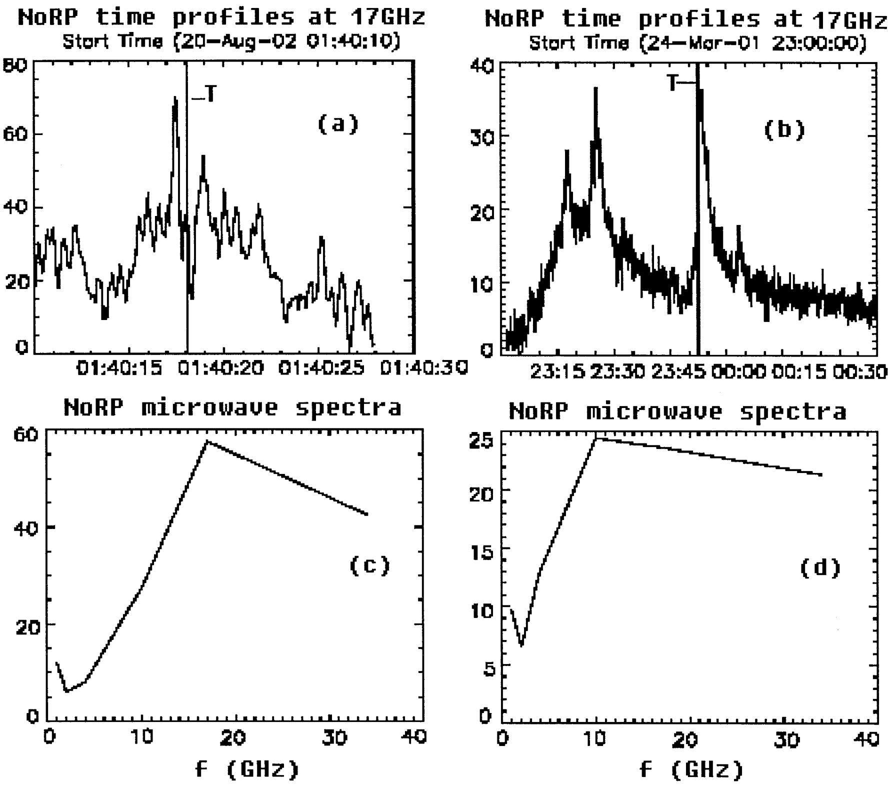

Figure 7. Similar to Figure 5, the *left* and *right panels* are for events 3 and 4, respectively.

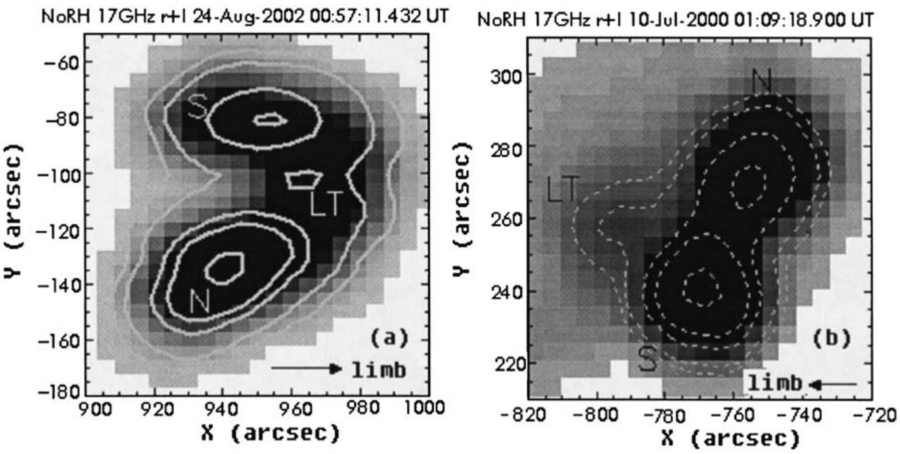

Figure 8. Stokes V (NoRH/17GHz) with contours overlaid on the NoRH/17GHz I image. The *solid and dashed lines* are for positive and negative V. (a) Event 1 contours: 5.e4, 1.e5, 5.e5, 1.e6, 3.e6. (b) Event 2 contours: −3.e4, −6.e4, −2.e5, −4.e5, −1.1e6.

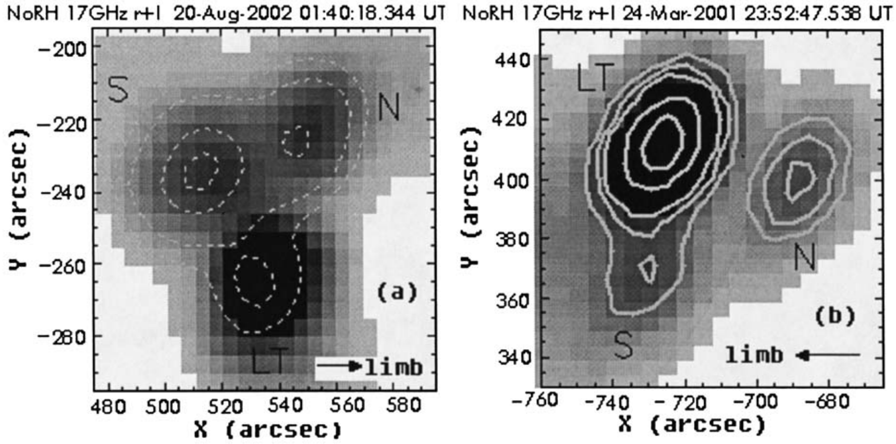

Figure 9. Similar to Figure 8. (a) Event 3 contours: −3.e4, −7.6e4, −4.5e5, −2.8e5. (b) Event 4 contours: 4.e4, 7.4e4, 1.2e5, 3.e5, 5.e5.

For the four events, a rough estimation of f_t is given using Equation (1). Assuming $N_e \sim 10^9$ electrons cm^{-3}, $S \sim 10^{10}$ cm, $B \sim 100$ G, we get $f_t \sim 3.2 \times 10^{10}$ Hz. Comparing this value with the observation frequency ($f = 1.7 \times 10^{10}$ Hz), the mode coupling should be weak.

3.2.2. *Type I*

For events 1, 2, the FP are always brighter than the LT at 17 GHz during the impulsive phase, which agrees with the well-known model given in Klein and Trottet (1984) and Paper I. The model predicts that the brightness peaks of optically thin emission are located near the FP of extended loops with a nonuniform magnetic field.

Event 1 is located near the west limb. Diskward and limbward are defined along the radial direction. Because this event occurred just near the limb, both footpoints seem to be located parallel to the solar limb, and it is very difficult to determine which footpoint is a diskward or a limbward one. So a probability is that the foot nearer the solar disk center by a bit is the diskward foot, the other one is the limbward foot. The angle θ is less than 90° for the diskward foot, because the polarity of the magnetic field is positive, thus the intrinsic sense of polarization is RCP corresponding to e-mode emission. For the limbward foot θ is greater than 90° corresponding to the negative polarity of the magnetic field. Then the intrinsic sense of polarization is LCP for e-mode emission. The emission of the limbward foot may cross the QT region with weak wave coupling in the lower corona. Thus the sense of polarization will be inverted to RCP. θ is greater than 90° for the LT, the situation is similar to the limbward foot. Finally the sense of polarization is RCP for the three sources in event 1.

Event 2 is located near the east limb, the heliocentric distance is about 57°. Both footpoints seem to be parallel to the solar limb. But if we see the underlying magnetic field in Figure 1(b) , the negative magnetic field, in which the south footpoint is situated, is located in the inner side of the positive magnetic field in which the north footpoint is situated, so the south footpoint may refer to the diskward foot and the other is the limbward foot. Corresponding to the underlying negative and positive magnetic field, $\theta > 90°$ and $\theta < 90°$ for the diskward foot and limbward foot, thus the intrinsic sense of polarization is LCP and RCP for *e*-mode emission, respectively. Similar to event 1, the limbward foot will suffer polarization inversion, and the polarization sense becomes LCP. Similar to the limbward foot, θ is less than 90° for the LT, finally the sense of polarization is LCP.

3.2.3. *Type II*

The LT of events 3, 4 is brighter than the FP near the maximum time. Melnikov, Shibasaki, and Reznikova (2002) have also found a similar fact, which is explained by the perpendicular to magnetic field pitch-angle anisotropy of injected high-energy electrons, and the strong concentration of mildly relativistic electrons in the upper part of a magnetic flaring loop.

Event 3 is located about 34° away from the center of the solar disk. Corresponding to the underlying magnetic field, $\theta > 90°$ and $\theta < 90°$ for the diskward foot and the limbward foot which are polarized in the sense of LCP and RCP for *e*-mode emission, respectively. Similar to event 1, the limbward foot will suffer polarization inversion, and the polarization sense becomes LCP. Similar to the limbward foot, θ is less than 90° for the LT, the sense of polarization is LCP after inversion of polarization sense.

Event 4 is located near the east limb, about 53° away from the center of the solar disk. The situation of event 4 is similar to event 1. The intrinsic polarization sense is RCP and LCP for the diskward foot and limbward foot, corresponding to positive and negative magnetic field, respectively, for *e*-mode emission. θ is greater than 90° for the LT, and the intrinsic polarization sense is LCP. The emission of the limbward foot and LT may cross the QT region with weak coupling in the lower corona, then the polarization sense is inverted to RCP. So the polarization sense of the three sources is RCP.

4. Conclusion

Four microwave bursts presented in the previous sections have a loop-like structure. The selected bursts may be divided into two types according to the brightness temperature of the LT versus FP. The FP is brighter than the LT for events 1, 2 during the impulsive phase, which may be interpreted as the well-known model. The LT is brighter than the FP for events 3, 4 near the maximum time, and the interpretation given by Melnikov is possible. Another possibility for events 3, 4 is that the LT is close to the reconnection region similar to the Masuda flare, which will result in brighter LT and complicated time profiles. Both possibilities need further detailed investigation. The polarization sense of the LT and FP is the same in each given burst, which is interpreted as propagation effects which may result in the inversion of the polarization sense of the limbward foot and loop-top source for *e*-mode emission.

Acknowledgements

The authors wish to thank Dr Shibasaki and Dr Yokoyama for helpful discussions and providing the NoRH data. The authors also want to thank the team of NoRP, *Yohkoh*, SOHO, and TRACE for providing the valuable data of NoRP, *Yohkoh*/SXT, SOHO/MDI, and TRACE/EUV. This study is supported by the NFSC projects No.10273025, 10333030, and '973' program with No. G2000078403.

References

Alissandrakis, C. E. and Preka-Papadema, P.: 1984, *Astron. Astrophys.* **139**, 507 (Paper I).
Alissandrakis, C. E., Nindos, A., and Kundu, M. R.: 1993, *Solar Phys.* **147**, 343.
Bandiera, R.: 1982, *Astron. Astrophys.* **112**, 52.
Cohen, M. H.: 1960, *Astrophys. J.* **131**, 664.
Klein, K. L. and Trottet, G.: 1984, *Astron. Astrophys.* **141**, 67.
Lara, A., Gopalswamy, N., Kundu, M. R., Pérez Enríquez, R., Koshiishi, H., and Enome, S.: 1998, *Solar Phys.* **178**, 353.
Melnikov, V. F., Shibasaki, K., and Reznikova V. E.: 2002, *Astrophys. J.* **580**, L185.
Preka-Papadema, P. and Alissandrakis, C. E.: 1988, *Astron. Astrophys.* **191**, 365.
Ramaty, R.: 1969, *Astrophys. J.* **158**, 753.
Takakura, T.: 1972, *Solar Phys.* **26**, 151.
Takakura, T. and Scalise, E., Jr.: 1970, *Solar Phys.* **11**, 434.
Zheleznyakov, V. V. and Zlotnik, Y.: 1963, *Astron. Zh.* **40**, 633 (*Soviet Astron.* **7**, 485).